

Evolution of the parton dihadron fragmentation functions

A. Majumder¹ and Xin-Nian Wang¹

¹*Nuclear Science Division, Lawrence Berkeley National Laboratory
1 Cyclotron road, Berkeley, CA 94720*

(Dated: November 6, 2018)

Quark and gluon parton dihadron fragmentation functions and their evolution are studied in the process of e^+e^- annihilation. We provide definitions of such dihadron fragmentation functions in terms of parton matrix elements and derive the momentum sum rules and their connection to single hadron fragmentation functions. We parameterize results from the Lund Monte Carlo model JETSET as the initial conditions for the parton dihadron fragmentation functions at the scale $Q_0^2 = 2 \text{ GeV}^2$. The evolution equations for the quark and gluon fragmentation functions are solved numerically and the results at different higher scales Q^2 agree well with JETSET results. The importance of the input from the single fragmentation functions is pointed out.

PACS numbers: 12.38.Mh, 11.10.Wx, 25.75.Dw

I. INTRODUCTION

In the analysis of particle production from jets in e^+e^- annihilation or in $p + p(\bar{p})$ collisions, a primary observable is the single particle inclusive cross section. Within perturbative QCD (pQCD) and at leading-twist, the single particle inclusive cross section in e^+e^- annihilation can be proved to factorize into a calculable perturbative hard partonic part and a nonperturbative single inclusive fragmentation function [1]. In elementary particle collisions it is also possible to measure multiple particle production cross sections. This has led to the construction and study of multi-particle observables such as event shapes [2, 3]. These offer further insight into the substructure of jets produced in high energy particle collisions. In the analysis of jets produced in high energy heavy-ion collisions or in semi-inclusive deeply inelastic scattering (DIS) off large nuclei, however, the latter analysis is quite infeasible. Along with the single inclusive cross section another measurable quantity which may offer insight into the modification of jet properties in a medium are two high momentum particle correlations.

Dihadron correlations have indeed been measured recently in a variety of experiments. In the study of jet suppression in heavy-ion collisions, correlations between two high p_T hadrons in azimuthal angle are used to study the medium modification of jet structure in heavy-ion collisions at the Relativistic Heavy-ion Collider (RHIC) [4, 5]. While the back-to-back correlations are suppressed in central $Au + Au$ collisions, indicating large parton energy loss in the dense medium, the same-side correlations remain approximately the same as in $p + p$ and $d + Au$ collisions. This is to be contrasted with the large suppression observed in single inclusive spectra [6]. Two hadron correlations within the same jet are also measured in DIS off various nuclei at the HERMES experiment [7]. In such experiments the dihadron correlations surprisingly display minimal variation with the choice of nuclear target, even though the single inclusive production of leading hadrons are significantly suppressed with increasing

atomic number of the nuclear target [8]. Given the experimental kinematics of both experiments, this may be considered as an indication of parton hadronization outside the medium. However, since the same-side correlation corresponds to the two-hadron distribution within a single jet, the observed phenomenon is highly nontrivial.

To study systematically such phenomena, an extension of the single inclusive fragmentation formalism of QCD is required, to include correlations between pairs of particles produced in the same jet. Toward this end, we had proposed dihadron fragmentation functions in a recent paper [9]. In that effort, the double differential cross section for the same-side production of two hadrons in the e^+e^- annihilation was factorized into the well known hard cross section for $e^+ + e^- \rightarrow \gamma^* \rightarrow q\bar{q}$ and the quark dihadron fragmentation functions. The essential purpose of this fragmentation function is to measure the distribution of hadron pairs produced in the fragmentation of a hard quark.

As shown in the case of single hadron fragmentation functions [10], the medium modification of the fragmentation function due to multiple scattering and induced gluon radiation closely resembles that of radiative corrections due to gluon bremsstrahlung in vacuum. Therefore, it is important to understand first the QCD evolution of the dihadron correlations in quark and gluon jets in vacuum. In the last study [9], we had concentrated on the definition of the dihadron fragmentation functions and derived the Dokshitzer-Gribov-Lipatov-Altarelli-Parisi (DGLAP) evolution equations [11, 12, 13] for the non-singlet quark dihadron fragmentation function. In this paper, we will consider singlet quark and gluon dihadron fragmentation functions which will be directly relevant to the study of medium modification of jets in high-energy heavy-ion and DIS collisions. In addition, we will explore momentum sum rules for the dihadron fragmentation functions and their relationship to single hadron fragmentation functions.

In the factorized form for the inclusive hadron production cross section, the short distance parton cross section can be computed order by order as a series

in $\alpha_s(Q^2)$ for reactions with momentum transfer much higher above Λ_{QCD} . The long distance objects or the inclusive n -hadron fragmentation functions contain the non-perturbative information of parton hadronization [1, 9]. These fragmentation functions can be defined in an operator formalism [14, 15] and hence are valid beyond the perturbative theory. They however cannot be calculated perturbatively and have to be instead inferred from experiments. Since the definitions of these functions are universal or process independent, once measured in one process, *e.g.* e^+e^- annihilation, they can be applied to another, *e.g.* deep inelastic scattering or $p + p$ collisions, and therein lies the predictive power of pQCD. Yet another predictive power of pQCD rests in the fact that once these fragmentation functions are measured or given at one energy scale, they can be predicted for all other energy scales via the DGLAP evolution equations.

While hadronization of the out going quark and gluon jets is a non-perturbative phenomena, inclusive hadron production cross sections in e^+e^- collisions have turned out to be one of the many successful predictions of perturbative QCD [12, 16, 17]. To the best of our knowledge, however, measurements of dihadron fragmentation functions have not been performed in e^+e^- experiments. In the numerical study of the nonsinglet quark dihadron fragmentation functions in Ref. [9], we used a simple ansatz for the initial condition as $D_{NS}(z_1, z_2) = D(z_1) \times D(z_2)$, which at best was just a guess and, as we will show later, differ significantly from the inherent hadron correlations in a single jet. To facilitate a more accurate numerical study of the singlet quark and gluon dihadron fragmentation functions in this paper, we will parameterize the results of the Lund Monte Carlo model JETSET [19] which has successfully described many aspects of jet fragmentation in both e^+e^- and DIS experiments.

The remaining sections of this paper are organized as follows. In Sec. II we review the definition of the double hadron fragmentation function. We outline how such a function may be isolated in the expression for a double differential inclusive cross section. In Sec. III we derive and discuss various sum rules that are obeyed by the dihadron fragmentation functions and their connection to single hadron fragmentation functions. In Sec. IV we outline the derivation of the DGLAP [11, 12, 13] evolution equations for the quark and gluon dihadron fragmentation functions. The initial conditions for the dihadron fragmentation functions are extracted from JETSET at a scale Q_0 in Sec. V. They are then evolved numerically via the DGLAP evolution equations to different scales Q and compared to the result from JETSET. Finally in Sec. VI we discuss the results of our calculation and present our conclusions.

II. DIHADRON FRAGMENTATION FUNCTIONS

In this section, we will review the definition and properties of dihadron fragmentation functions in the semi-inclusive process $e^+ + e^- \rightarrow \gamma^* \rightarrow h_1 + h_2 + X$ via single jet fragmentation where two hadrons are identified. In most cases we will be concerned with back-to-back quark and antiquark jets. Study of the gluon fragmentation function, however, will involve three jet events. In both cases, our focus will always be on two hadrons produced in the same jet.

The cross section for the process of e^+e^- annihilation into hadrons may be expressed as

$$\begin{aligned} \sigma &= \frac{1}{2s} \frac{e^4}{4(q^2)^2} \sum_{S_{had}} \delta^4(k_1 + k_2 - P_S) \\ &\times \mathcal{L}_{\mu\nu} \langle 0 | J^\mu(0) | S_{had} \rangle \langle S_{had} | J^\nu(0) | 0 \rangle \\ &\equiv \frac{e^4}{2sq^4} \frac{\mathcal{L}_{\mu\nu} W^{\mu\nu}}{4}, \end{aligned} \quad (1)$$

where $J^\mu = \sum_q \bar{\psi}_q \gamma^\mu \psi_q$ is the hadronic electromagnetic current, $\mathcal{L}_{\mu\nu}$ the leptonic tensor and $W^{\mu\nu}$ the hadronic tensor. The four momentum of the virtual photon is $q = k_1 + k_2 \equiv (Q, 0, 0, 0)$ and the Mandelstam variable $s = q^2 = Q^2$. In the remaining, the sum over S_{had} will include both the sum over the complete set of states and the phase space integration $\Pi_{f \in S_{had}} d^3p_f / 2E_f (2\pi)^3$ and $P_S = \sum_f p_f$.

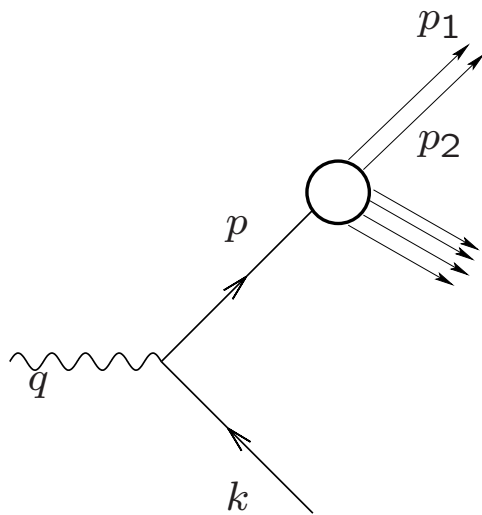


FIG. 1: The leading order Feynman diagram contributing to the double inclusive fragmentation function.

The definition and factorization of dihadron fragmentation functions involve identifying two hadrons with nearly parallel momenta p_1 and p_2 among hadronic states along the direction of one of the partons and replacing the remaining sum over hadronic states with a sum over

the rest of all partonic states (see Fig. 1). This is followed by an extraction of the leading twist component (see Ref. [9] for details). Differentiating the total inclusive cross section with respect to the forward momentum fractions of the two hadrons *i.e.*, z_1, z_2 , the leading order (LO) factorized form of the double differential cross section may be expressed as

$$\frac{d^2\sigma}{dz_1 dz_2} = \sum_q \sigma_0^{q\bar{q}} \left[D_q^{h_1 h_2}(z_1, z_2) + D_{\bar{q}}^{h_1 h_2}(z_1, z_2) \right], \quad (2)$$

where $\sigma_0^{q\bar{q}}$ is the total LO hard cross section for an e^+e^- pair to annihilate into hadrons. The two functions $D_q^{h_1 h_2}(z_1, z_2)$ and $D_{\bar{q}}^{h_1 h_2}(z_1, z_2)$ represent the dihadron fragmentation functions for a quark and an antiquark. The quark dihadron fragmentation function in light-cone gauge ($A^+ = 0$ gauge) is obtained as,

$$D_q^{h_1, h_2}(z_1, z_2) = \frac{z_h^4}{4z_1 z_2} \int \frac{d^2 q_\perp}{4(2\pi)^3} \int \frac{d^4 p}{(2\pi)^4} \times T_q(p; p_1, p_2) \delta\left(z_h - \frac{p_h^+}{p^+}\right). \quad (3)$$

The forward momentum fractions of the identified hadrons z_1, z_2 are $z_1 = p_1^+/p^+$ and $z_2 = p_2^+/p^+$. The momentum p_h represents the sum of the hadronic momenta *i.e.*, $p_h = p_1 + p_2$. Henceforth, the direction identified by \vec{p}_h will be considered the same as the direction of the jet. The transverse spread of the two hadrons around the jet direction is indicated by the relative transverse momentum $\vec{q}_\perp = \vec{p}_{1\perp} - \vec{p}_{2\perp}$. As is indicated by the final δ -function in the above equation, the momentum fraction $z_h = z_1 + z_2$. The matrix element of the operator product $T_q(p; z_1, z_2)$ is given as (in the light-cone gauge)

$$T_q(p; p_1, p_2) = \text{Tr} \left[\frac{\gamma^+}{2p_h^+} \int d^4 x e^{ip \cdot fx} \sum_{S-2} \times \langle 0 | \psi_q(x) | p_1, p_2, S-2 \rangle \langle p_1, p_2, S-2 | \bar{\psi}_q(0) | 0 \rangle \right]. \quad (4)$$

The above expression for the dihadron fragmentation functions includes the integration over the transverse momenta q_\perp . As a result the angular correlation between the detected hadrons is also integrated over in such a definition. In order to observe such correlation a differentiation of the dihadron fragmentation function with respect to the transverse angle must be carried out. In this paper, we will continue to focus on the integrated fragmentation function.

The above definition for the dihadron fragmentation function also admits a simple diagrammatic interpretation in terms of the cut-vertex method of Mueller [14]. The diagrammatic rule in terms of the quark cut-vertex is outlined in Fig. 2. The product of these rules along with the factor $z_h^4/(4z_1 z_2)$ is the integrated dihadron fragmentation function.

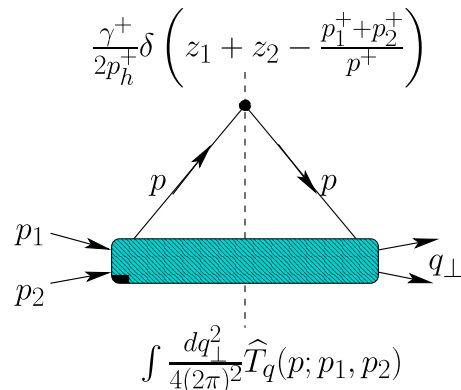


FIG. 2: The cut-vertex representation of the quark dihadron fragmentation function.

The gluon dihadron fragmentation function can be similarly constructed by identifying two hadrons moving with almost parallel momenta in the direction of the outgoing gluon in a three jet event in e^+e^- annihilation processes. Factorizing the hard cross section from the soft matrix element one obtains the gluon dihadron fragmentation function at leading twist as (see Ref. [9] for details),

$$D_g(z_1, z_2) = \frac{z_h^3}{2z_1 z_2} \int \frac{dq_\perp^2}{8(2\pi)^2} \int \frac{d^4 l}{(2\pi)^4} \times \delta\left(z_h - \frac{p_h^+}{l^+}\right) T_g(l; p_1, p_2). \quad (5)$$

In the above equation, the meanings of various momenta and forward momentum fractions are the same as for the quark dihadron fragmentation function. The gluon overlap matrix element $T_g(l; p_1, p_2)$ is defined as

$$T_g(l; p_1, p_2) = \int d^4 x e^{il \cdot x} \sum_{S-2} \langle 0 | A_\mu^a(x) | p_1, p_2, S-2 \rangle \times \langle p_1, p_2, S-2 | A_\nu^b(0) | 0 \rangle \frac{\delta^{ab} d^{\mu\nu}(l)}{16}, \quad (6)$$

where $d^{\mu\nu}(l)$ is the gluon's polarization tensor in the light-cone gauge and sum over the color indices of the gluon field is implied.

The gluon dihadron fragmentation function also admits a simple diagrammatic interpretation in terms of the cut-vertex method. The diagrammatic rule in terms of the gluon cut-vertex is outlined in Fig. 3. The product of these rules along with the factor $z_h^2/(2z_1 z_2)$ is the integrated dihadron fragmentation function.

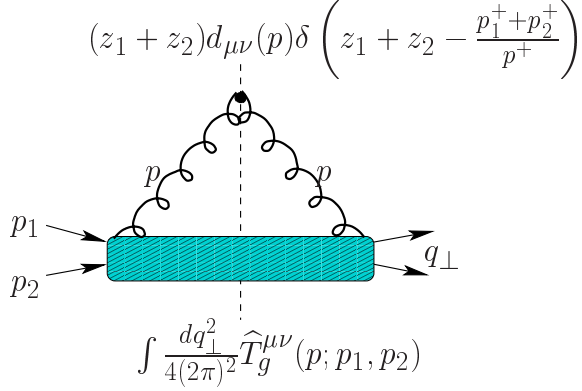


FIG. 3: The cut-vertex representation of the gluon dihadron fragmentation function.

III. SUM RULES

One of the many interesting properties obeyed by the single inclusive fragmentation functions are the various sum rules. Primary among them are the momentum sum rules

$$\sum_h \int dz z D_q^h(z) = \sum_h \int dz z D_g^h(z) = 1. \quad (7)$$

Here the single inclusive fragmentation functions are defined as [14, 20, 21],

$$D_q^h(z) = \frac{z^3}{2} \int \frac{d^4 p}{(2\pi)^4} \delta\left(z - \frac{p_h^+}{p^+}\right) T_q(p, p_h); \quad (8)$$

$$D_g^h(z) = z^2 \int \frac{d^4 l}{(2\pi)^4} \delta\left(z - \frac{p_h^+}{l^+}\right) T_g(p, p_h), \quad (9)$$

in terms of parton matrix elements

$$T_q(p, p_h) = \text{Tr} \left[\frac{\gamma^+}{2p_h^+} \int d^4 x \sum_{S-1} \langle 0 | \psi_q(0) | p_h, S-1 \rangle \right. \\ \left. \times \langle p_h, S-1 | \bar{\psi}_q(x) | 0 \rangle e^{ip \cdot x} \right]; \quad (10)$$

$$T_g(l, p_h) = \int d^4 x \sum_{S-1} \langle 0 | A_\mu^a(x) | p_h, S-1 \rangle \\ \times \langle p_h, S-1 | A_\nu^b(0) | 0 \rangle \frac{\delta^{ab} d^{\mu\nu}(l)}{16} e^{il \cdot x}. \quad (11)$$

They can be interpreted as single inclusive hadron multiplicity distributions within fractional momentum z_h and $z_h + dz_h$ from parton fragmentation. Similarly, one can derive the momentum sum rules for dihadron fragmentation functions. Furthermore, one can also derive sum

rules that relate dihadron fragmentation functions to single fragmentation functions.

Given $\vec{p}_{\perp h} = \vec{p}_{\perp 1} + \vec{p}_{\perp 2}$ and $\vec{q}_{\perp} = \vec{p}_{\perp 1} - \vec{p}_{\perp 2}$, we have assumed that the total transverse momentum of the two hadrons $\vec{p}_{\perp h}$ is parallel to the parton's transverse momentum in the definition of parton dihadron fragmentation functions in Eqs. (3) and (5). Similarly, if we consider single hadron fragmentation, the hadron transverse momentum $\vec{p}_{\perp,1}$ is also parallel to the partons transverse momentum. We should then have the following identity,

$$\int \frac{d^2 p_{\perp h}}{2\pi z_h^2 p_q^{+2}} = \int \frac{d^2 p_{\perp 1}}{2\pi z_1^2 p_q^{+2}} = 1, \quad (12)$$

which is just integration over the angle of the initial parton. Using the above identity, one can recast the momentum integration as,

$$\frac{dz_2}{z_2} d^2 p_{\perp h} \frac{d^2 q_{\perp}}{4(2\pi)^3} = 2d^2 p_{\perp 1} \frac{d^3 p_2}{2E_2(2\pi)^3}. \quad (13)$$

Here, the external quark momentum is p_q^+ and hadrons momenta are $p_1^+ = z_1 p_q^+$ and $p_2^+ = z_2 p_q^+$. One can also rewrite the δ -function $\delta(z_h - p_h^+/p^+) = (z_1/z_h)\delta(z_1 - p_1^+/p^+)$ in the definition of the dihadron fragmentation functions.

Since a dihadron fragmentation function is essentially a two-hadron multiplicity distribution, its sum rules must involve the information of the number of hadron pairs. An example of this is

$$\sum_{h_1, h_2} \int dz_1 dz_2 D_{q,g}^{h_1 h_2}(z_1, z_2) = \langle N(N-1) \rangle, \quad (14)$$

where $\langle N(N-1) \rangle$ is the second cumulant moment of the multiplicity distribution and

$$\langle N \rangle = \sum_h \int dz D_{q,g}^h(z) \quad (15)$$

is the mean multiplicity from parton fragmentation. Inside the parton matrix elements of the fragmentation function, one can rewrite

$$\sum_{h_2, S-2} \int \frac{d^3 p_2}{2E_2(2\pi)^3} |p_1, p_2, S-2\rangle \langle p_1, p_2, S-2| \\ = \sum_{h_2} \int \frac{d^3 p_2}{2E_2(2\pi)^3} \hat{a}_{h_1}^\dagger(p_1) \hat{a}_{h_2}^\dagger(p_2) \hat{a}_{h_2}(p_2) \hat{a}_{h_1}(p_1), \\ = \hat{a}_{h_1}^\dagger(p_1) \hat{a}_{h_1}(p_1) (\hat{N} - 1) \quad (16)$$

where \hat{a}_h^\dagger and \hat{a}_h are creation and annihilation operators for hadron h , and

$$\hat{N} = \sum_h \int \frac{d^3 p}{2E(2\pi)^3} \hat{a}_h^\dagger(p) \hat{a}_h(p), \quad (18)$$

is the total multiplicity operator. Here we have assumed hadrons as bosons. Using similar expression,

$$\sum_{S-1} |p_1, S-1\rangle \langle p_1, S-1| = \hat{a}_{h_1}^\dagger(p_1) \hat{a}_{h_1}(p_1), \quad (19)$$

for single inclusive states, one can effectively have the identity,

$$\begin{aligned} & \sum_{h_2, S-2} \int \frac{d^3 p_2}{2E_2(2\pi)^3} |p_1, p_2, S-2\rangle \langle p_1, p_2, S-2| \\ &= \frac{\langle N(N-1) \rangle}{\langle N \rangle} \sum_{S-1} |p_1, S-1\rangle \langle p_1, S-1|. \end{aligned} \quad (20)$$

Using Eqs. (12), (13) and (20), one can obtain the following relationship,

$$\sum_{h_2} \int dz_2 D_{q,g}^{h_1 h_2}(z_1, z_2) = \frac{\langle N(N-1) \rangle}{\langle N \rangle} D_{q,g}^{h_1}(z_1), \quad (21)$$

between dihadron and single hadron fragmentation functions. Using the momentum sum rules for the single hadron fragmentation functions, one has the following momentum sum rule for dihadron fragmentation functions,

$$\sum_{h_1, h_2} \int dz_1 dz_2 \frac{z_1 + z_2}{2} D_{q,g}^{h_1 h_2}(z_1, z_2) = \frac{\langle N(N-1) \rangle}{\langle N \rangle}. \quad (22)$$

Note that both $\langle N \rangle$ and $\langle N(N-1) \rangle$ in Eqs. (14) and (15) are not infrared safe and therefore not well defined in the collinear approximation for the fragmentation functions. Consequently, these sum rules for dihadron fragmentation functions are also not well defined in collinear approximation. They, however, may provide useful phenomenological constraints for practical modeling of these fragmentation functions where collinear approximation might not be required.

IV. DGLAP EVOLUTION

One of the many successes of the factorized pQCD is the prediction of the scaling violation of the single inclusive fragmentation functions via the DGLAP equations. If the fragmentation functions are measured at an initial large scale $Q_0 \gg \Lambda_{QCD}$, they can be predicted at any higher scale Q . In terms of the physical pictures afforded by the parton model, one imagines that the initiating quark loses its large virtuality through the radiation of multiple soft gluons and finally fragment into hadrons. Such a picture is validated within field theory by considering the leading twist contributions of higher order diagrams in e^+e^- annihilation. The leading log (LL) contributions from all such diagrams are resummed and a set of coupled differential equations for the rate of change of the fragmentation functions with the momentum scale is derived.

In Ref. [9], a QCD evolution equation for the non-singlet quark dihadron fragmentation function in an operator formalism was derived. The resulting evolution equation also admits a simple physical interpretation in terms of the diagrams shown in Figs. 4, 5, 6. The reader will note the new contribution from the diagram indicated in Fig. 6: the two detected hadrons emerging from the fragmentation of two separate partons. This contribution will turn out to be essential in determining the QCD evolution of dihadron fragmentation functions.

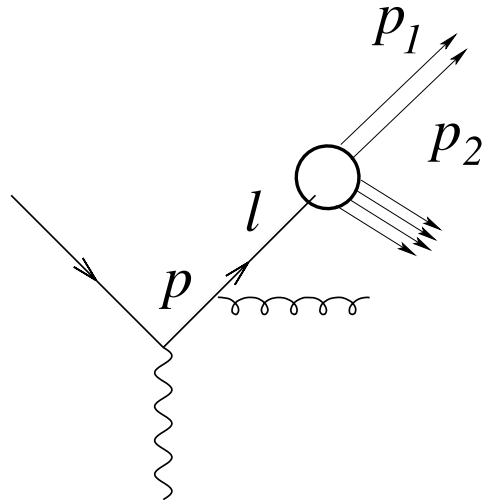


FIG. 4: The contribution from the quark fragmentation to the NLO correction of the quark dihadron fragmentation function.

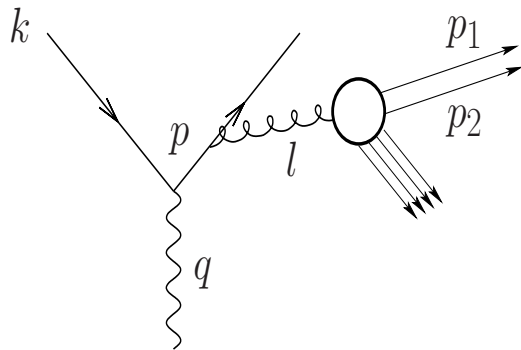


FIG. 5: The contribution of gluon fragmentation to the NLO correction of the quark dihadron fragmentation function.

The resulting DGLAP evolution equation for the quark dihadron fragmentation function is given as

$$\begin{aligned}
\frac{\partial D_q^{h_1 h_2}(z_1, z_2, Q^2)}{\partial \log Q^2} = & \frac{\alpha_s}{2\pi} \left[\int_{z_1+z_2}^1 \frac{dy}{y^2} P_{q \rightarrow qg}(y) D_q^{h_1 h_2} \left(\frac{z_1}{y}, \frac{z_2}{y}, Q^2 \right) \right. \\
& + \int_{z_1}^{1-z_2} \frac{dy}{y(1-y)} \hat{P}_{q \rightarrow qg}(y) D_q^{h_1} \left(\frac{z_1}{y}, Q^2 \right) D_g^{h_2} \left(\frac{z_2}{1-y}, Q^2 \right) \\
& + \int_{z_2}^{1-z_1} \frac{dy}{y(1-y)} \hat{P}_{q \rightarrow qg}(y) D_q^{h_2} \left(\frac{z_2}{y}, Q^2 \right) D_g^{h_1} \left(\frac{z_1}{1-y}, Q^2 \right) \\
& \left. + \int_{z_1+z_2}^1 \frac{dy}{y^2} P_{q \rightarrow gq}(y) D_g^{h_1 h_2} \left(\frac{z_1}{y}, \frac{z_2}{y}, Q^2 \right) \right]. \quad (23)
\end{aligned}$$

Where $D_q^h(z, Q^2)$ and $D_g^h(z, Q^2)$ are the single inclusive quark and gluon fragmentation functions, and $D_g^{h_1 h_2}(z_1, z_2, Q^2)$ is the gluon dihadron fragmentation function [see Eq. (5)]. In the above equation $P_{q \rightarrow qg}(y)$ is the splitting function for a quark to radiate off a gluon and keep a fraction y of its initial forward light-cone momentum. It is identical to the splitting function kernel of the DGLAP equation for the single fragmentation function, *i.e.*,

$$P_{q \rightarrow qg}(y) = C_F \left(\frac{1+y^2}{1-y} \right)_+. \quad (24)$$

The subscript ‘+’ indicates that the negative virtual correction has been added within the splitting function. The splitting function in the second line of Eq. (23), $\hat{P}_{q \rightarrow qg}$, is identical to the above equation except that it lacks the negative virtual correction. The last splitting function is the probability for a quark to radiate off a gluon with a fraction y of its forward momentum and has an expression identical to the case for the single fragmentation case. It should be pointed out in passing that $P_{q \rightarrow gq}(y)$ also has no virtual correction and thus no negative contribution. In the evolution of the dihadron fragmentation function the sole negative contribution arises from the virtual piece in $P_{q \rightarrow qg}(y)$; all other contributions are positive. Another difference from the case of the single inclusive fragmentation function are the measures $1/y^2$ and $1/y(1-y)$. These can be understood on the basis that the origin of the dihadron fragmentation function lies in the evaluation of a double differential inclusive cross section (see Sec. II of Ref. [9]). We also point out that Eq. (23) may also be derived in the cut-vertex formalism via the renormalization of the bare cut-vertex presented in Fig. 2.

The evolution of the gluon dihadron fragmentation function may be derived in the cut-vertex formalism via the renormalization of the bare cut-vertex shown in Fig.

3. It should be pointed out that the evolution equations for the quark and gluon dihadron fragmentation functions may be motivated using parton model arguments

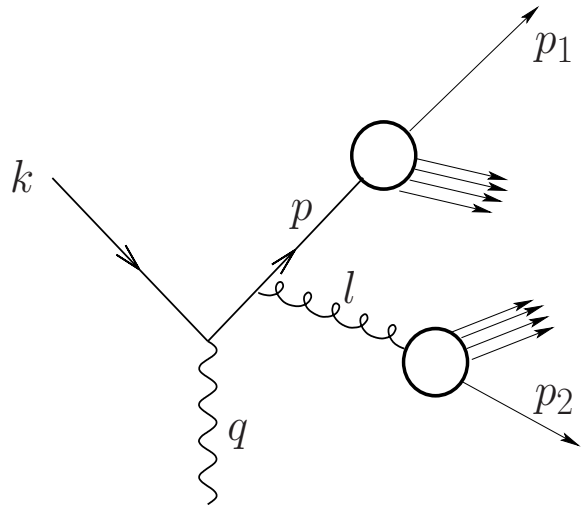


FIG. 6: The mixed contribution to the NLO correction of the quark dihadron fragmentation function.

such as those of Refs. [17, 22]. The evolution equation for the gluon dihadron fragmentation functions now includes four pieces: the gluon may split into a quark-antiquark pair or into two gluons. The detected hadrons may both emanate from the same parton (quark, antiquark or gluon) or from the two different partons resulting from the split, *i.e.*,

$$\begin{aligned}
\frac{\partial D_g^{h_1 h_2}(z_1, z_2, Q^2)}{\partial \log Q^2} &= \frac{\alpha_s}{2\pi} \left[\int_{z_1+z_2}^1 \frac{dy}{y^2} 2n_f P_{g \rightarrow q\bar{q}}(y) D_q^{h_1 h_2} \left(\frac{z_1}{y}, \frac{z_2}{y}, Q^2 \right) \right. \\
&+ \int_{z_1}^{1-z_2} \frac{dy}{y(1-y)} n_f P_{g \rightarrow q\bar{q}}(y) D_q^{h_1} \left(\frac{z_1}{y}, Q^2 \right) D_{\bar{q}}^{h_2} \left(\frac{z_2}{1-y}, Q^2 \right) \\
&+ \int_{z_2}^{1-z_1} \frac{dy}{y(1-y)} n_f P_{g \rightarrow q\bar{q}}(y) D_q^{h_2} \left(\frac{z_2}{y}, Q^2 \right) D_{\bar{q}}^{h_1} \left(\frac{z_1}{1-y}, Q^2 \right) \\
&+ \int_{z_1+z_2}^1 \frac{dy}{y^2} P_{g \rightarrow gg}(y) D_g^{h_1 h_2} \left(\frac{z_1}{y}, \frac{z_2}{y}, Q^2 \right) \\
&\left. + \int_{z_1}^{1-z_2} \frac{dy}{y(1-y)} \hat{P}_{g \rightarrow gg}(y) D_g^{h_1} \left(\frac{z_1}{y}, Q^2 \right) D_g^{h_2} \left(\frac{z_2}{1-y}, Q^2 \right) \right]. \quad (25)
\end{aligned}$$

In the above equation, n_f is the number of flavors of quarks assumed. In the remainder of this paper we will assume n_f to be 3. Henceforth, the quark and antiquark fragmentation functions will not be distinguished; in both cases the singlet fragmentation function will be assumed *i.e.*, $D_q = D_{\bar{q}} = (D_q + D_{\bar{q}})/2$. The splitting function $P_{g \rightarrow q\bar{q}}$ is the probability for the initial gluon to decay into a quark-antiquark pair with the quark carrying a fraction y of the forward momentum of the gluon. It is given as,

$$P_{g \rightarrow q\bar{q}} = T_F(y^2 + (1-y)^2), \quad (26)$$

where T_F is the Casimir. It may be noted that interchanging quark and antiquark may also be achieved by the switch $y \rightarrow 1-y$. In Eq. (25), $P_{g \rightarrow gg}(y)$ is the probability for the gluon to split into two gluons, and has the expression

$$\begin{aligned}
P_{g \rightarrow gg}(y) &= 2C_A \left[\frac{y}{(1-y)_+} + \frac{1-y}{y} + y(1-y) \right] \\
&+ \delta(1-y) \left[\frac{11}{6}C_A - \frac{2}{3}n_f T_F \right]. \quad (27)
\end{aligned}$$

The presence of the ‘+’-function as well as the δ -function is the result of virtual contributions from gluon and quark-antiquark loops. The final splitting function in Eq. (25) is essentially the above splitting function without the virtual corrections, *i.e.*,

$$\hat{P}_{g \rightarrow gg}(y) = 2C_A \left[\frac{y}{(1-y)} + \frac{1-y}{y} + y(1-y) \right], \quad (28)$$

since there are no virtual corrections to the independent fragmentation contributions at the same order. As hadrons with finite momentum fractions originating from both gluons are detected, the range of values of the intermediate momentum fraction y may approach neither 0 nor 1. Therefore, there is no infrared divergence even without cancellation by virtual corrections. As one can

see now there exist two new contributions to the evolution of the gluon dihadron fragmentation function: from independent single fragmentation functions after a split to a quark-antiquark and to two gluons. Both these contributions are positive. This again will turn out to be an essential part in the equation that influences the QCD evolution of gluon dihadron fragmentation functions.

V. RESULTS OF EVOLUTION: COMPARISON WITH EVENT GENERATORS

To date, measurements of single inclusive cross sections in e^+e^- collisions remain the primary set of data used in the parameterization of the fragmentation functions and testing their scaling violations. In many ways this provides an independent justification of the factorized pQCD approach to high energy collisions. The absence of any initial state interactions makes e^+e^- experiments ideal for baseline measurements of parton fragmentation in vacuum, while allowing for tractable calculations of their evolution. However, no such measurements have been performed for double inclusive cross sections. In the absence of such measurements and in the interest of simplicity we turn to Monte Carlo event generators for both the extraction of the initial conditions and for comparison to the numerical results of the evolution equation for dihadron fragmentation functions.

Monte Carlo event generators such as JETSET [19] have enjoyed great success as simulators of e^+e^- collision events. They provide reliable predictions not only for single inclusive measurements but also for many-particle observables such as event shape and inter-jet particle flows. Hence, it is reasonable to assume that two particle correlations extracted from a ‘‘tuned’’ event generator will closely mimic such correlations measured in real experiments. The events generated will be restricted to two-jet events for a measurement of the quark dihadron fragmentation function and to three-jet events for the gluon dihadron fragmentation function. Single inclusive hadron

fragmentation functions for both quarks and gluons will also be measured in the same set of events.

In the extraction of the quark fragmentation functions three million dijet events distributed equally over three flavors were simulated using JETSET. The \sqrt{s} of the reaction was set to 20 GeV. In all such events the direction of the initiating quark and its initial virtuality were controlled. The virtuality of the initiating quark Q sets the scale of the fragmentation function. The forward light-cone momentum of the initiating quark was read off from the event list. In such experiments the single fragmentation function is defined as

$$D_q(z) = \frac{1}{N_{evt}} \frac{dN(z)}{dz}. \quad (29)$$

In this paper, we restrict the flavor of the detected particles to π^+ and π^- . The variable $z = p_\pi^+/p_q^+$, where p_q is the momentum of the fragmenting quark. The denominator N_{evt} is the number of events, whereas $dN(z)$ represents the number of particles, over all events, that fall between z and $z+dz$ of the momentum fraction. The dihadron fragmentation function is measured as

$$D_q(z_1, z_2) = \frac{1}{N_{evt}} \frac{d^2P(z_1, z_2)}{dz_1 dz_2}, \quad (30)$$

where, $d^2P(z_1, z_2)$ represents the number of pairs of pions with momentum fractions between $(z_1, z_1 + dz_1)$ and $(z_2, z_2 + dz_2)$. In constructing these functions, z_1 was always restricted to be larger than z_2 .

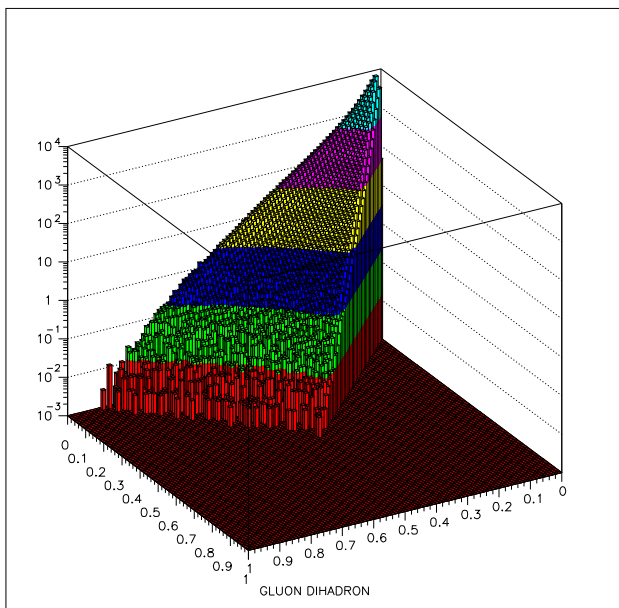


FIG. 7: The gluon dihadron fragmentation function.

For the extraction of the gluon fragmentation function, an identical procedure as above was carried out with the sole restriction, that all events be three-jet events and a large fraction of the energy be concentrated in the gluon.

The latter requirement guarantees that events are predominantly composed of cases where the gluon and the quark antiquark pair are always contained in opposite hemispheres. Tracking the final hadrons in the gluon's hemisphere lead to the construction of the gluon fragmentation function. It should be pointed out that in the Lund model of fragmentation, which is the underlying fragmentation model in JETSET, an out going gluon is represented by a kink in the fragmenting string which begins at the quark and terminates at the antiquark. Perturbative showers within JETSET modify this picture and allow for multiple strings to form and fragment. A plot of the gluon dihadron fragmentation function thus extracted is shown in Fig. 7.

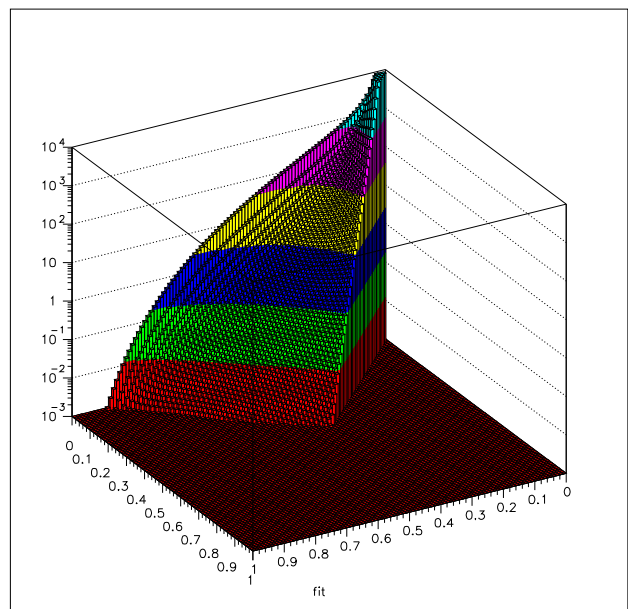


FIG. 8: The result of χ^2 fit of the function of Eq. (31) to Fig. 7.

For the convenience of providing initial conditions to the evolution equations, the fragmentation function of Fig. 7 is parametrized by fitting to a function of the type:

$$D(z_1, z_2) = N z_1^{\alpha_1} z_2^{\alpha_2} (z_1 + z_2)^{\alpha_3} (1 - z_1)^{\beta_1} (1 - z_2)^{\beta_2} \times (1 - z_1 - z_2)^{\beta_3}. \quad (31)$$

There are seven parameters in the above fit: $N, \alpha_1, \alpha_2, \alpha_3, \beta_1, \beta_2, \beta_3$. The reader will note that the structure of the function is a simple generalization of the parameterization of the single fragmentation functions. The fit is carried out by the method of minimum logarithm of χ^2 . The logarithm ensures that the fit is better at larger values of z_1 and z_2 . A plot of the final result of the fit for the gluon dihadron fragmentation function is shown in Fig. 8. One notes that the fit function of Eq. (31) mimics the function closely except at very small z_1 and z_2 . This is unimportant as in the

evolution we will always restrict our attention away from very small z_1 and z_2 . We will not explicitly show the quark dihadron fragmentation function and its fit here. Suffice to say that the fit is even better for the quark, which, as is the case for the single fragmentation function, generically has a harder spectrum in momentum fraction. Values for the various parameters of the fits to the quark and gluon fragmentation functions at the two different values of the Q^2 used in this paper are presented in table I.

One unique feature of the DGLAP evolution equations for dihadron fragmentation functions is that the equations couple dihadron to single hadron fragmentation functions. The single hadron fragmentation functions themselves evolve independently according to their own DGLAP evolution equations. We find that the single hadron fragmentation functions obtained from JETSET simulations can be described very well by Binneswies-Kniehl-Kramer(BKK) parameterization [23] of the actual experimental data. Therefore, in our numerical study of the evolution equations for dihadron fragmentation functions, we will simply use the BKK parameterization for the single hadron fragmentation functions and their evolution with the momentum scale Q .

The fit function shown in Fig. 8 as well as its analogue for the quark will provide the initial conditions to the differential equations outlined in Eqs. (25) and (23) respectively. In both cases, the initial scale of the fragmentation functions is set to $Q_0^2 = 2 \text{ GeV}^2$. This corresponds to $\log(Q_0^2) = 0.693$. These are shown as the filled triangles for the quarks and the filled squares for the gluons in Fig 9. We have chosen a fixed $z_1 = 0.5$ and let z_2 vary from 0 to $1 - z_1$, since several experiments that measure medium modification of the dihadron fragmentation functions, which we will discuss in separate studies, have similar kinematic range. Note the orders of magnitude difference between the two distributions. This feature holds for most of the range of z_1 and z_2 except at very small momentum fractions where the gluon fragmentation function overtakes that of the quark.

Similar to the procedure carried out in Ref. [9] for non-singlet quark dihadron fragmentation functions, results of the evolution will be presented in increments of $\log(Q^2) = 1$. As expected, we note a softening of the spectrum with rising scale. We terminate the evolution at $\log(Q^2) = 4.693$, corresponding to scale $Q^2 = 109 \text{ GeV}^2$. To compare the results of the evolution equations in Eqs.(23) and (25) to Monte Carlo event simulations, dihadron fragmentation functions at the highest scale are once again extracted from JETSET. The number of events used to sample the fragmentation functions and the method of the fit remain identical to the case at lower Q^2 described above. The results are presented as open triangles for the quarks and open squares for the gluons. As shown they are in excellent agreement with the results of the evolution equations. This provides the most crucial test of the evolution equations we have presented in this paper.

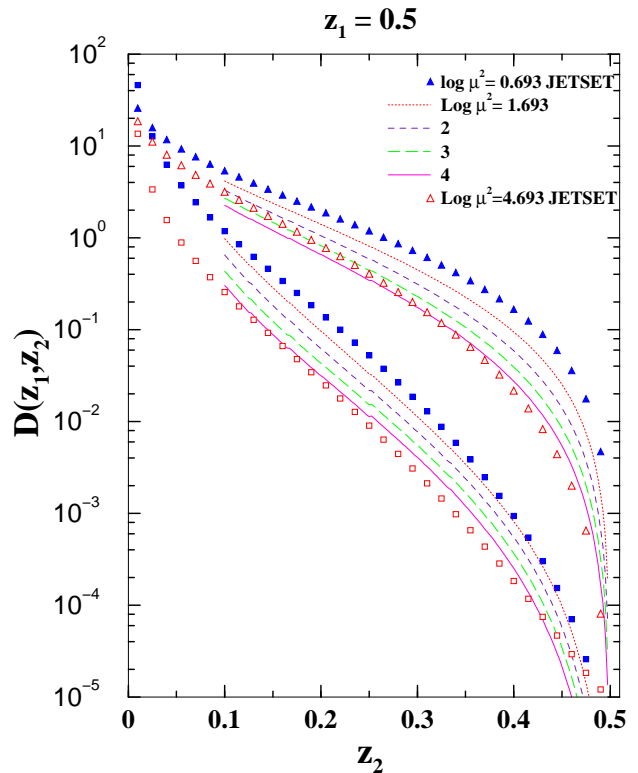


FIG. 9: Results of the evolution of the quark and gluon fragmentation function ($D_q(z_1, z_2), D_g(z_1, z_2)$). In all cases z_1 is held fixed at 0.5.

Parton Q^2	N	α_1	α_2	α_3	β_1	β_2	β_3
quark 2 GeV ²	4.080	-0.673	-0.440	-0.707	0.196	1.717	1.359
quark 109 GeV ²	5.872	-1.103	-0.425	-0.436	0.410	2.997	2.164
gluon 2 GeV ²	8.000	-6.246	-1.319	6.736	4.324	15.214	1.351
gluon 109 GeV ²	1.090	-8.848	-1.430	8.568	6.216	22.031	-0.145

TABLE I: Values of different parameters used in the fit to the fragmentation functions.

In the recent experimental studies *e.g.*, two high p_T particle production in $p+p$, $p+A$ and $A+A$ collisions at RHIC, or two particle correlation in inclusive DIS by the HERMES experiment, one usually measures dihadron correlations in the form of inclusive spectra of associated particles produced in correlation with a high momentum trigger hadron. These measurements are essentially the ratios of the number of trigger and associated particle pairs divided by the number of triggers. They are equivalent to the ratios of the dihadron fragmentation functions to the single fragmentation functions. This quantity is plotted in Fig. 10 for the same range of scales as that in Fig. 9. The value of z_1 is once again held fixed at 0.5. The

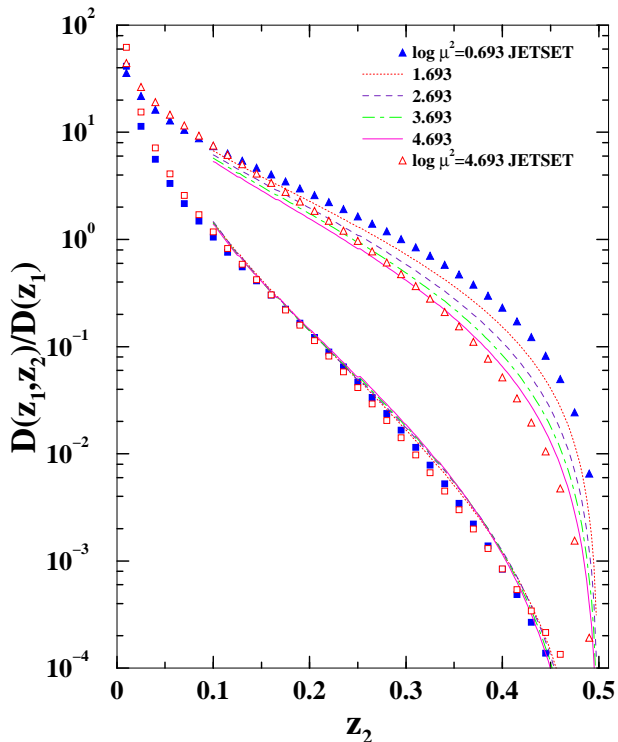


FIG. 10: Results of the evolution of the ratio of the dihadron fragmentation function to the single fragmentation function for quarks and gluons.

single hadron fragmentation functions are given by BKK parameterization [23] at same Q^2 which can also be derived from the same Monte Carlo simulations or evolved with the DGLAP equations for single hadron fragmentation functions. We have checked that all three methods give almost identical results. While it may come as no surprise that the evolution of this ratio is also predicted by the dihadron DGLAP evolution equations, it must be pointed out that the ratio of the dihadron and single hadron fragmentation functions do not display substantial change with variation of the scale. This is especially true for the gluon fragmentation function.

VI. DISCUSSIONS AND CONCLUSIONS

In this study, a very general discussion of the properties of the dihadron fragmentation functions has been carried out. Various results have been outlined: the momentum sum rules have been discussed, evolution equations for both the singlet quark and gluon dihadron fragmentation functions have been derived and solved numerically, comparisons with results from Monte Carlo event generators (in the absence of experimental measurements) are made. Very good agreement has been obtained from such comparisons. In the remaining, we cast a backward glance at dihadron fragmentation functions, summariz-

ing the sentinel points of the aforementioned analysis, and present an overview of future studies.

Factorization ensures that fragmentation functions are well defined and universal. Once defined and measured in a given process they must admit the same definition and hence numerical value in another experiment. Such definitions in light-cone gauge were presented in Ref. [9] in LO of QCD. Gauge invariance of the definition is apparent and the generalization involves little more than the similar procedure invoked in the case of the single inclusive fragmentation function [1]: The partonic operators at two space time points were connected by a Wilson line of the gauge field. In the case of the gluon fragmentation function, the gluon vector potential was replaced with gauge invariant field operators.

Single inclusive fragmentation functions, which have the interpretation of single inclusive hadron distributions, obey well defined sum rules. The momentum sum rules for the dihadron fragmentation functions, which have the interpretation of the pair multiplicity in a jet, have been derived in Sec. III. One can relate the dihadron to single hadron fragmentation functions through these sum rules. However, they will involve first and second order cumulant moments of the multiplicity distribution since dihadron fragmentation functions involve pair multiplicity. The appearance of the cumulant moments makes the sum rules for dihadron fragmentation functions less rigorous since they are not well defined in the collinear factorization approximation. However, in practice, they will provide useful guidance for phenomenological modeling of the dihadron fragmentation functions.

Though fragmentation functions are well defined in terms of parton matrix elements, yet they still involve non-perturbative objects. Therefore, the exact form of a fragmentation function may not be estimated purely from QCD. They, however, can be measured at a given energy scale for a whole set of continuous forward momentum fractions. Once such a measurement is made, one may derive the value at any other higher scale via the evolution equations in pQCD. Comparing these with experimental results at higher scales amounts to a test of the QCD evolution equations. In this paper, the lack of experimental results was circumvented by the use of the JETSET event generator which is tuned to fit a variety of experimental data on e^+e^- annihilation. Note that event generators can reproduce not only the single inclusive measurements in e^+e^- events, but also a multitude of many particle observables. We used dihadron fragmentation functions from JETSET simulations at the scale of $Q_0 = 2 \text{ GeV}^2$ as the initial condition for the DGLAP evolution equations. We demonstrated that the results at higher scales, *e.g.*, $Q^2 = 109 \text{ GeV}^2$ from the numerical solution to the evolution equations are in excellent agreement with that extracted from JETSET simulations at the same scale, as shown in Figs. 9 and 10. This comparison provided a stringent test to the new evolution equations presented in this study.

The effect and validity of each component of the

DGLAP equations may be further tested by a simple exercise. The various terms presented in Eqs. (23) and (25) may be broadly divided into two categories. The regular components, which we call *correlated* two hadron fragmentation, are contained in the first and last lines of Eq. (23) and the first and fourth lines of Eq. (25). These are simple generalizations of the single inclusive DGLAP equations and depend solely on dihadron fragmentation functions. The new components, which we call *independent* two hadron fragmentation, make up the second and third line of Eq. (23) and the second, third and last line of Eq. (25). These depend on products of single inclusive fragmentation functions, and therefore couple the evolution of the dihadron fragmentation functions with that of the single fragmentation functions. We may compute the evolution of dihadron fragmentation functions without the contribution from the components of independent fragmentation. This leads to the results presented in Fig. 11. As the reader may note, the calculated evolution is now a poorer fit to the results from JETSET. While this may not be very noticeable for the quark fragmentation function, the gluon fragmentation function which is at least an order of magnitude smaller than the quark fragmentation function shows a very noticeable difference. The evolution of the gluon fragmentation function depends on two separate pieces of independent fragmentation. One receives contributions from the product of two gluon single fragmentation functions, while another from the product of a quark and an antiquark distribution functions. It is the removal of latter that produces the majority of the difference in the evolution of the gluon dihadron fragmentation function between Fig. 9 and Fig. 11. This is due to the fact that we restrict our attention to large z where the quark fragmentation function dominates over the gluon, and the product of two single quark fragmentation functions is larger than the gluon dihadron fragmentation function at large z_1 and z_2 . Thus each component of the evolution has a role to play in the change of the fragmentation function from one scale to another. The contributions from the new components of independent fragmentation are always positive. Therefore, they slow down the scale evolution of the dihadron fragmentation functions, particularly for gluon jets at large z_1 and z_2 . This is also the reason why the triggered distributions (the ratio between dihadron and single hadron fragmentation functions) change very little with the scale for gluon jets as shown in Fig. 9.

With the question of evolution of the dihadron fragmentation functions set aside, we now focus on certain general properties of the fragmentation function as has been exposed by this analysis. It may be noted from Fig. 10 that the ratio of the dihadron fragmentation function to the single fragmentation function of the leading hadron ($D_q^{h_1 h_2}(z_1, z_2, Q^2)/D_q^{h_1}(z_1, Q^2)$) shows little change as a function of Q^2 even as $Q^2 \rightarrow 100 \text{ GeV}^2$. This is especially true of the ratio in the case of the gluon fragmentation function, which shows practically no change

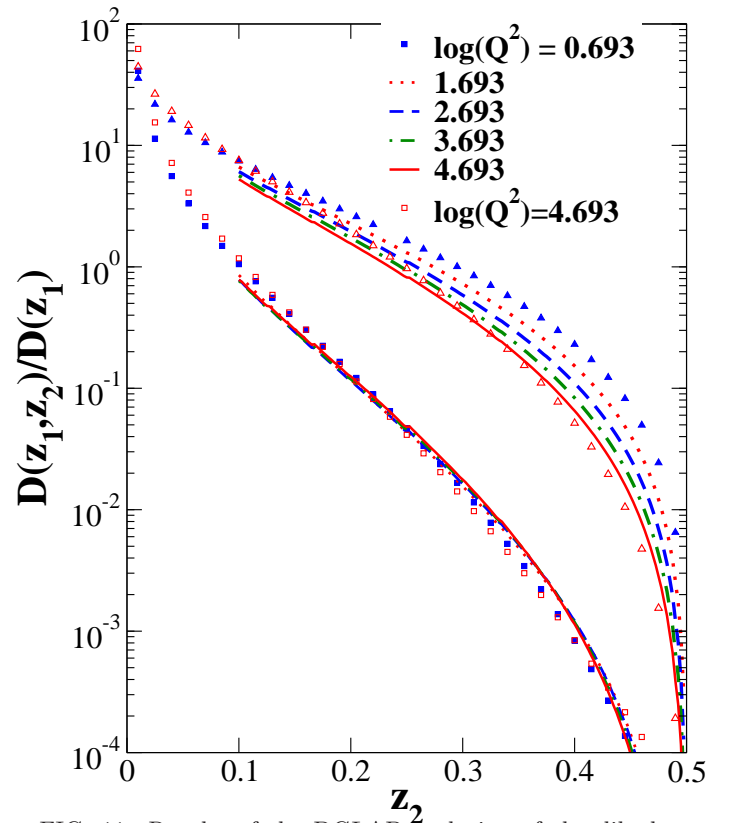


FIG. 11: Results of the DGLAP evolution of the dihadron fragmentation function without the independent fragmentation terms. All parameters are the same as Fig. 9.

with Q^2 over the range of z_1 and z_2 explored. The results of evolution are strongly dependent, however, on the initial conditions and thus on the actual values of z_1 and z_2 . This is consistent with the observations noted in our previous study of quark non-singlet dihadron fragmentation functions [9].

In recent experiments at RHIC [4], correlations of two high p_\perp hadrons have been measured in $p+p$, $d+Au$ and $Au+Au$ collisions. Hadrons with $p_\perp \geq 4 \text{ GeV}$ are used as a trigger. Once such a “leading” particle is identified, the experiment measures the differential probability of the “next-to-leading” hadrons or associated high p_\perp particles emanating from the same collision with transverse momentum in the range $2 < p_\perp < 4 \text{ GeV}$ at a given azimuthal angle ϕ with respect to the direction of the leading particle. In Ref. [4], results for $dN/d\phi/N_{trig}$ are measured. While a large suppression was noted for $\phi \approx \pi$ (away-side) in central collisions, almost no change was seen in the vicinity of $\phi \approx 0$ (near side). Assuming both hadrons (leading and associated) with the same-side correlation come from fragmentation of a jet, the initial jet energy is at least about 7 to 10 GeV. This is about the same range of momentum scale we have considered in studying the evolution of dihadron fragmentation functions. This range of Q^2 is also relevant to the experiments of DIS on nuclei [7], where medium modification of the ratio of the dihadron fragmentation function to the

single fragmentation function of the leading hadron was reported. A double ratio of the above quantity R_A/R_D with a large nucleus versus that in deuteron showed minimal change with the atomic number. A complete understanding of the relevance of this observation requires a repeat of the calculation presented in this article with the inclusion of a medium modification. While the study with medium modification will be presented in a forthcoming article, we can already see the trend by analyzing the analogous effects of QCD evolution in the vacuum.

If the results of Ref. [4] for $dN/d\phi/N_{trig}$ are integrated over the angle ϕ in the vicinity of $\phi = 0$, one should obtain, in effect, the ratio of the dihadron fragmentation function to the single fragmentation function. This is, no doubt, based on the assumption that both the leading and the next-to-leading particles emerge from the same parent parton. In the results of Ref. [4] the ratio is essentially integrated from $z_2 \approx 0.3$, $z_1 \approx 0.6$ to $z_2 \approx 0.4$, $z_1 \approx 0.4$. Within this kinematic range, there is not much change of the ratio of the fragmentation functions as a function of the Q^2 due to gluon bremsstrahlung in vacuum. Therefore, it may not be entirely surprising that no variation was noted in the same side two hadron correlations in Ref. [4] due to medium induced gluon bremsstrahlung, in particular if one takes into account the trigger bias caused by parton energy loss [24].

It has been pointed out recently that the ratio of the dihadron fragmentation function to the single fragmentation function of the leading hadron (*i.e.*, $D(z_1, z_2)/D(z_1)$) may be numerically similar to the single fragmentation function of the associated hadron *i.e.*, $D(z_2)$ [25]. This was noted experimentally and in simulations. We point out that there is indeed some truth to this observation. In Fig. 12 we plot the ratios of the dihadron fragmentation function to the fragmentation function of the leading hadron for the quark and gluon. This is compared with the single inclusive fragmentation functions of a quark (solid lines) and gluon (dashed lines). In the range $0 < z_2 < 0.3$, the single inclusive fragmentation functions do indeed closely approximate the ratio $D_q(z_1, z_2)/D_q(z_1)$. This fact is however only true for the quark; no such similarity is noted for the gluon. The primary reason for the difference between $D_q(z_2)$ and $D_q(z_1, z_2)/D_q(z_1)$ for $z_2 > 0.3$ is the differences in kinematic bounds experienced by the two quantities: $D_q(z_2) \rightarrow 0$ as $z_2 \rightarrow 1$ whereas $D_q(z_1, z_2) \rightarrow 0$ as $z_2 \rightarrow 1 - z_1$. In Fig. 12, z_1 is held fixed at 0.5, thus the maximum value of $z_2 = 0.5$. This differences in kinematic bounds may be circumvented by considering a rescaled single fragmentation function $D_q(z_2/(1 - z_1))/(1 - z_1) = 2D_q(2z_2)$ which experiences a similar kinematic bound as $D_q(z_1, z_2)/D_q(z_1)$ for $z_1 = 0.5$. This rescaled function is represented by the dot-dashed lines in Fig. 12 which is very similar to $D_q(z_1, z_2)/D_q(z_1)$ with the same momentum scale Q .

Finally, we point out that in the derivation of results presented in this paper, we depended on the assumption that the energy scales of the processes in question were

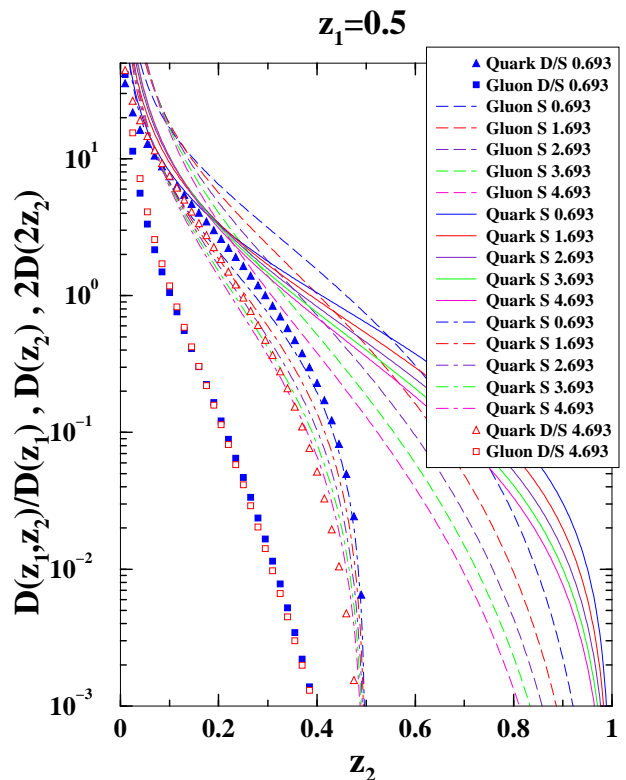


FIG. 12: Comparisons between the ratio of the dihadron fragmentation function to the single fragmentation functions of the leading hadron (indicated as D/S) and the fragmentation function of the associated hadron (indicated as S). The D/S curves are the same as in Fig. 10. The single fragmentation functions are obtained from the BKK parameterization of Ref. [23]. The dashed lines are for the gluon and the solid lines represent a rescaled quark fragmentation function $2D_q^{h_2}(2z_2)$. The Q^2 of a particular dot-dashed line is the same as the Q^2 of the solid line in the same order.

high enough for the applicability of pQCD methods. We also required the fragmentation functions to be defined at a scale larger than a semihard scale μ_\perp , such that $\Lambda_{QCD}^2 \ll \mu_\perp^2 \ll Q^2$. This semi-hard scale μ_\perp restricts the relative transverse momentum between hadrons such that they are considered as from one parton jet. We thus required Q^2 to be high enough for a hierarchy of scales to exist. The evolution equations are applicable solely when this hierarchy of scales exists.

Acknowledgments

The authors wish to thank E. Wang for many helpful discussions. This work was supported in part by the Natural Sciences and Engineering Research Council of Canada, and in part by the Director, Office of Science, Office of High Energy and Nuclear Physics, Division of Nuclear Physics, and by the Office of Basic En-

ergy Sciences, Division of Nuclear Sciences, of the U.S. Department of Energy under Contract No. DE-AC03-

76SF00098.

-
- [1] J. C. Collins, D. E. Soper, and G. Sterman, in *Perturbative Quantum Chromodynamics* edited by A. Mueller, (World Scientific 1989), and references therein.
- [2] R. K. Ellis, D. A. Ross and A. E. Terrano, Phys. Rev. Lett. **45**, 1226 (1980).
- [3] S. Catani, G. Turnock, B. R. Webber and L. Trentadue, Phys. Lett. B **263**, 491 (1991).
- [4] C. Adler *et al.* [STAR Collaboration], Phys. Rev. Lett. **90**, 082302 (2003) [arXiv:nucl-ex/0210033].
- [5] S. S. Adler *et al.* [PHENIX Collaboration], arXiv:nucl-ex/0408007.
- [6] K. Adcox *et al.* [PHENIX Collaboration], Phys. Rev. Lett. **88**, 022301 (2002) [arXiv:nucl-ex/0109003]; C. Adler *et al.* [STAR Collaboration], Phys. Rev. Lett. **89**, 202301 (2002) [arXiv:nucl-ex/0206011].
- [7] P. Di Nezza [HERMES Collaboration], J. Phys. G **30**, S783 (2004).
- [8] A. Airapetian *et al.* [HERMES Collaboration], Eur. Phys. J. C **20**, 479 (2001) [arXiv:hep-ex/0012049].
- [9] A. Majumder and X. N. Wang, Phys. Rev. D **70**, 014007 (2004) [arXiv:hep-ph/0402245].
- [10] X. F. Guo and X. N. Wang, Phys. Rev. Lett. **85**, 3591 (2000) [arXiv:hep-ph/0005044]; X. N. Wang and X. F. Guo, Nucl. Phys. A **696**, 788 (2001) [arXiv:hep-ph/0102230]; J. Osborne and X.-N. Wang, Nucl. Phys. A **710**, 281 (2002) [arXiv:hep-ph/0204046]; B. W. Zhang and X.-N. Wang, Nucl. Phys. A **720**, 429 (2003) [arXiv:hep-ph/0301195].
- [11] V. N. Gribov and L. N. Lipatov, Yad. Fiz. **15**, 781 (1972) [Sov. J. Nucl. Phys. **15**, 438 (1972)].
- [12] Yu. L. Dokshitzer, Sov. Phys. JETP **46**, 641 (1977) [Zh. Eksp. Teor. Fiz. **73**, 1216 (1977)].
- [13] G. Altarelli and G. Parisi, Nucl. Phys. B **126**, 298 (1977).
- [14] A. H. Mueller, Phys. Rev. D **18**, 3705 (1978).
- [15] A. Majumder, J. Phys. G **30**, S1305 (2004) [arXiv:hep-ph/0404292].
- [16] G. Sterman and S. Weinberg, Phys. Rev. Lett. **39**, 1436 (1977).
- [17] R. D. Field and R. P. Feynman, Nucl. Phys. B **136**, 1 (1978).
- [18] M. Gyulassy and M. Plumer, Phys. Lett. B **243**, 432 (1990); X. N. Wang and M. Gyulassy, Phys. Rev. Lett. **68**, 1480 (1992).
- [19] B. Andersson, G. Gustafson, G. Ingelman and T. Sjostrand, Phys. Rept. **97**, 31 (1983); T. Sjostrand, arXiv:hep-ph/9508391.
- [20] A. H. Mueller, Phys. Rept. **73**, 237 (1981).
- [21] J. A. Osborne, E. Wang and X. N. Wang, Phys. Rev. D **67**, 094022 (2003) [arXiv:hep-ph/0212131].
- [22] R. D. Field, *Applications of Perturbative QCD*, Addison-Wesley, New York (1995).
- [23] J. Binnewies, B. A. Kniehl and G. Kramer, Phys. Rev. D **52**, 4947 (1995) [arXiv:hep-ph/9503464].
- [24] X. N. Wang, Phys. Lett. B **579**, 299 (2004) [arXiv:nucl-th/0307036].
- [25] J. Y. Jia, arXiv:nucl-ex/0409024, *Proc. of Hot Quarks 2004*, J. Phys. G. *to appear*; private communication.